

Self-consistent analysis of high-temperature effects on InGaAsP/InP lasers

Joachim Piprek, Patrick Abraham, and John E Bowers

Department of Electrical and Computer Engineering, University of California at Santa Barbara, Santa Barbara, CA 93106-9560, USA

Abstract. We evaluate temperature effects on threshold current and slope efficiency of 1.55 μm Fabry-Perot lasers between 20°C and 120°C. Experimental results are analyzed using the commercial laser simulator PICS3D. The software self-consistently combines two-dimensional carrier transport, heat flux, strained quantum well gain computation, and optical wave guiding with a longitudinal mode solver. All relevant physical mechanisms are considered, including their dependence on temperature and local carrier density. Careful adjustment of material parameters leads to an excellent agreement between simulation and measurements at all temperatures. At lower temperatures, Auger recombination controls the threshold current. At high temperatures, vertical electron leakage from the separate confinement layer mainly limits the laser performance. The increase of internal absorption is less important. However, all these carrier and photon loss enhancements with higher temperature are mainly triggered by the reduction of the optical gain.

1. Introduction

The strong temperature sensitivity of InP-based long-wavelength laser diodes has been investigated for more than two decades [1]. However, the dominating physical mechanisms are still under discussion. In recent years, this discussion includes Auger recombination, intervalence band absorption (IVBA), thermionic carrier emission from the active region, lateral carrier spreading, passive layer absorption, spontaneous recombination within passive layers, and optical gain reductions. Different physical mechanisms govern in different temperature regions with a critical transition temperature [2]. It was recently found that the non-uniformity of the MQW carrier distribution strongly affects the differential internal efficiency of long-wavelength multi-quantum well (MQW) lasers [3]. For the first time, we present a numerical analysis of light vs. current measurements that considers all of the above physical mechanisms and their interaction self-consistently.

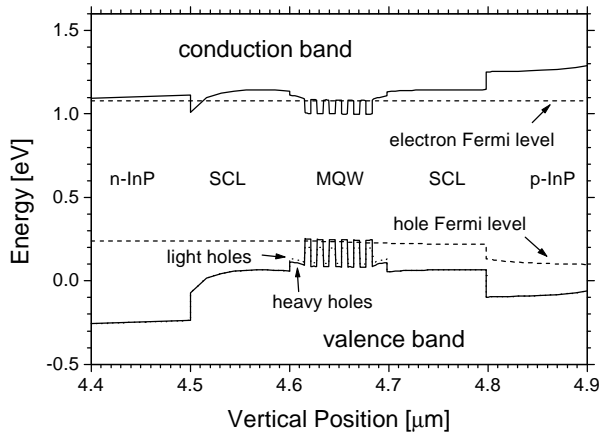


Fig. 1: Energy band diagram of our strained InGaAsP/InP active region.

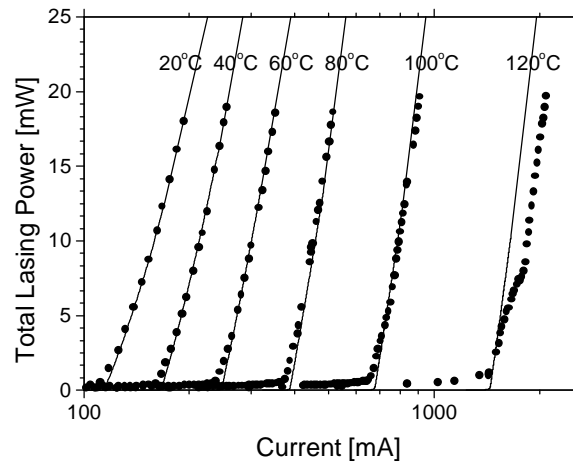


Fig. 2: Measurement (dots) and simulation (lines) of pulsed laser characteristics.

2. Laser structure and experimental results

We measured the high-temperature performance of broad-area Fabry-Perot InGaAsP/InP ridge-waveguide laser diodes emitting at 1.55 μm wavelength. The MQW active region contains six 6.4nm thick quantum wells with 1% compressive strain (Fig. 1). The 5.5nm thick barriers exhibit slight tensile strain (0.04%). The MQW stack is sandwiched between undoped InGaAsP separate confinement layers (SCLs) for vertical waveguiding. Broad area ridge-waveguide lasers with 57 μm wide stripes are processed. The lasers are characterized as cleaved. The average facet power reflectivity is assumed to be 0.28. Lasers with 269 μm cavity length are primarily used in our analysis.

Light power vs. current (LI) curves are measured under pulsed conditions (0.05 % duty cycle) to prevent self-heating. The device temperature is increased by heating the copper stage from room temperature (20 $^{\circ}\text{C}$) up to 120 $^{\circ}\text{C}$. The thermal red-shift of the emission wavelength is $d\lambda/dT = -0.54\text{nm/K}$ due to the shift of the gain peak. Temperature effects on our pulsed LI characteristics are shown in Fig. 2 (dots). The characteristic temperature T_0 of the threshold current decreases from 55K at room temperature to 20K at 110 $^{\circ}\text{C}$. Similarly, the characteristic temperature of the slope efficiency shows a monotonic change from -180K to -30K. The physical mechanisms behind these temperature effects are analyzed by numerical simulation [4].

3. Laser model and material parameters

We utilize an advanced laser software [5], which self-consistently combines 2D carrier transport, heat flux, optical gain computation, and wave guiding within the transversal plane (x,y) with a mode solver in longitudinal direction (z). The drift-diffusion model of carrier transport includes Fermi statistics and thermionic emission at hetero-barriers. Vertical carrier

leakage is mainly controlled by the offset of conduction band (ΔE_c) and valence band (ΔE_v) at the hetero-barrier. We find best agreement with the measurements by using a band offset ratio of $\Delta E_c / \Delta E_v = 0.4 / 0.6$ which is typical for the InGaAsP/InP system. Both the vertical and the lateral leakage currents plus all recombination currents within active (QW) and passive layers of the waveguide region add up to the injection current. The QW spontaneous recombination rate is calculated self-consistently from energy band structure and Fermi distribution. For Auger recombination, we assume an activation energy of 60 meV (CHHS process) [6] which leads to an excellent agreement between simulation and measurements (Fig. 2). The fit gives a room-temperature CHHS Auger parameter of $1.6 \times 10^{-28} \text{ cm}^{-6} \text{ s}^{-1}$.

The conduction bands in our strained QWs are assumed to be parabolic and the non-parabolic valence bands are computed by the 4×4 **kp** method including valence band mixing [7]. The local optical gain is calculated self-consistently from the local Fermi distribution of carriers at each bias point of the LI curve. A Lorentzian broadening function is used with 0.1ps intraband relaxation time. Band gap shrinkage due to carrier-carrier interaction is considered as $\Delta E_g = -\xi N^{1/3}$ with $\xi = 10^{-8} \text{ eV cm}$. The thermal band gap reduction parameter $dE_g/dT = -0.28 \text{ meV/K}$ is extracted from the measured thermal shift of the lasing wavelength. Figure 3 plots the peak gain as function of the carrier density at different temperatures. Rising temperatures cause a wider Fermi spreading of carriers lowering the optical gain. Carrier density and injection current need to be increased to maintain the required threshold gain. This is the main trigger mechanism for the observed temperature sensitivity of the threshold current.

The local absorption coefficient is proportional to the density of electrons (n) and holes (p): $\alpha = \alpha_b + k_n n + k_p p$. The small background loss coefficient α_b represents carrier-density independent mechanisms like photon scattering at defects. Free-carrier absorption due to electrons is known to be negligible in $1.55\mu\text{m}$ InGaAsP/InP lasers ($k_n = 10^{-18} \text{ cm}^2$). Mainly due to IVBA, holes dominate the absorption in our lasers and the fit to LI measurements in Fig. 2 gives $k_p = 82 \times 10^{-18} \text{ cm}^2$. This number is governed by quantum well contributions.

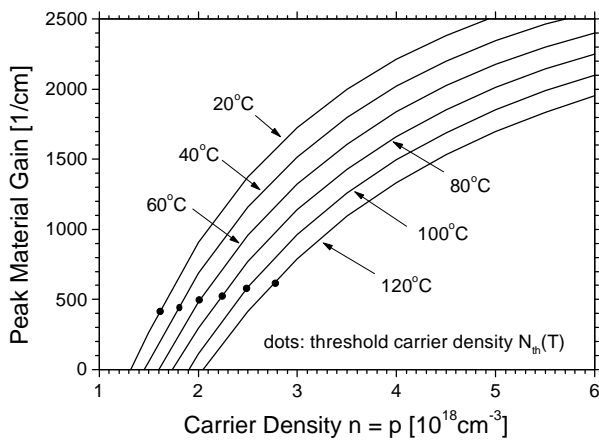


Fig. 3 Calculated peak gain vs. carrier density at different temperatures.

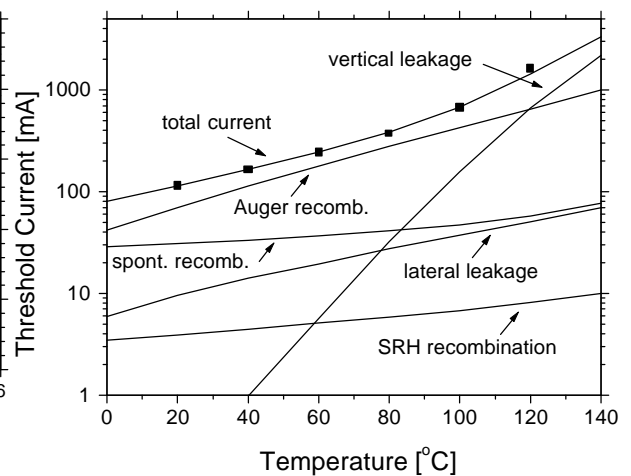


Fig. 4 Simulated threshold current and its components vs. temperature (dots: measurement).

4. Analysis of measurements

Figure 4 plots the pulsed threshold current and its components as function of temperature. At room temperature, the strongest contribution to the total threshold current comes from QW Auger recombination (61%), followed by spontaneous emission (27%), lateral leakage current (8%), and Shockley-Read-Hall (SRH) recombination (3%). At 120°C, vertical electron leakage into p-InP becomes the dominant carrier loss mechanism (47%), leaving behind Auger recombination (45%), spontaneous emission (4%), lateral leakage (3%), and SRH recombination (1%). All these calculated contributions add up perfectly to the measured threshold currents (dots in Fig. 4). Its temperature sensitivity is dominated by Auger recombination at lower temperatures and by vertical leakage at higher temperatures. These carrier loss mechanisms strongly depend on density and distribution of electrons and holes. Gain reductions with temperature elevation (Fig. 3) trigger higher carrier densities and higher losses.

Absorption is governed by the density of holes which is the highest in the quantum wells. At room temperature, 64% of the internal optical loss occurs within the quantum wells and 10% within barriers and SCLs. The remaining 26% originate in the p-InP cladding layer which hosts a considerable part of the guided wave. At 120°C, the quantum wells cause 60% of the internal absorption whereas the contribution of barriers and SCLs rises to 24%. The total absorption doubles within this temperature range. Thus, absorption by unconfined carriers rises strongly with temperature elevation. However, passive layer absorption does not dominate the temperature sensitivity of our long-wavelength lasers, as suggested by other authors [2].

5. Conclusion

The self-consistent simulation of temperature effects on gain, carrier density, recombination, leakage, and absorption allows for a full explanation of the measured temperature sensitivity of 1.55 μm InGaAsP/InP MQW laser diodes. None of these physical mechanisms can be neglected. One-sided models lead to one-sided interpretations of measurements and contribute to the controversy in this field. Different types of laser diodes may exhibit different balances of these mechanisms. However, advanced numerical models help to extract detailed physical information from laser measurements and improve the understanding of temperature effects.

References

- [1] Suematsu Y and Adams A R (eds.) 1994 *Handbook of Semiconductor Lasers and Photonic Integrated Circuits* (London: Chapman & Hall)
- [2] Seki S, Oohashi H, Sugiura H, Hirono T, and Yokoyama K 1996 *IEEE J. Quantum Electron.* **32** 1478-86
- [3] Piprek J, Abraham P, and Bowers J E 1999 *Appl. Phys. Lett.* **74** 489-91
- [4] Piprek J, Abraham P, and Bowers J E, *submitted to IEEE J. Quantum Electron.*
- [5] PICS3D 4.1.2 by Crosslight Software 1998 (www.crosslight.ca)
- [6] Seki S, Lui W W, and Yokoyama K 1995 *Appl. Phys. Lett.* **66** 3093-5
- [7] Chuang S L 1991 *Phys. Rev. B* **43** 9649-61